Available online at www.sciencedirect.com

ScienceDirect

Energy Procedia 92 (2016) 317 – 325

Energy Procedia

6th International Conference on Silicon Photovoltaics, SiliconPV 2016

Improved silicon surface passivation of APCVD Al_2O_3 by rapid thermal annealing

Lachlan E. Black[a,*], Thomas Allen[b], Keith R. McIntosh[c], Andres Cuévas[b]

[a]*Department of Applied Physics, Eindhoven University of Technology, Eindhoven 5612, The Netherlands*
[b]*Research School of Engineering, The Australian National University, Canberra ACT 0200, Australia*
[c]*PV Lighthouse, Coledale NSW 2515, Australia*

Abstract

Short-duration post-deposition thermal treatments at temperatures above those normally used for annealing activation have the potential to further improve the already excellent passivation of crystalline silicon (c-Si) achieved by Al_2O_3, but have so far received little attention. In this work we investigate the influence of rapid thermal annealing (RTA) on the surface passivation of c-Si by Al_2O_3 deposited by atmospheric pressure chemical vapour deposition (APCVD) as a function of RTA peak temperature between 500 and 900°C, and for Al_2O_3 deposition temperatures between 325 and 440°C. The saturation current density J_0 of undiffused *p*-type surfaces is observed either to increase or decrease following RTA depending on the Al_2O_3 deposition temperature and the RTA peak temperature. The optimum deposition temperature depends on the post-deposition thermal processing to be applied. Films deposited at lower temperatures provide worse passivation after low temperature heat treatment, but maintain this passivation better at higher RTA temperatures. An exceptionally low J_0 of 7 fA cm^{-2}, due to the combination of a very low interface state density D_{it} and unusually high negative fixed charge density Q_f, is achieved by the use of a short 500–550°C RTA combined with optimised deposition conditions.

Peer review by the scientific conference committee of SiliconPV 2016 under responsibility of PSE AG.

Keywords: surface passivation; aluminium oxide; crystalline silicon; chemical vapour deposition; rapid thermal annealing.

* Corresponding author.
E-mail address: l.e.black@tue.nl

Peer review by the scientific conference committee of SiliconPV 2016 under responsibility of PSE AG.
doi:10.1016/j.egypro.2016.07.088

1. Introduction

Effective surface passivation is essential for the realization of high-efficiency photovoltaic devices based on crystalline silicon. In the last decade Al_2O_3 has emerged to become the gold standard in silicon surface-passivation, providing unprecedented passivation especially of *p*-type surfaces [1]. It is well-established that for Al_2O_3 films deposited at lower temperatures, some post-deposition thermal treatment is generally required to "activate" the surface passivation. This typically takes the form of an extended (10–30 minute) anneal at 400–450°C in N_2 or forming gas. Thermal treatments at higher temperatures have been shown to sometimes degrade, and sometimes improve the surface passivation. Generally, investigations of the effects of higher temperature processing have employed either extended (~10–30 minute) anneals at moderate temperatures (usually <600°C) [2]–[6], intended to activate the passivation, or relatively short (several seconds), high-temperature (~800°C) treatments intended to simulate the contact-"firing" process employed in conventional Si solar cell manufacturing [6]–[11], in which the goal is to demonstrate the stability of the existing passivation.

There appear to be few reported investigations of the effects of very short (~1 s) thermal treatments at moderate temperatures. However, previous work indicates a complex response of Al_2O_3 passivation to thermal processing depending on both temperature and exposure time, as well as Al_2O_3 deposition parameters. In particular, it appears that Al_2O_3 passivation may not always improve or degrade monotonically with increasing annealing time at higher temperatures, but may reach an optimum at some shorter annealing time and subsequently degrade [11]. This suggests that a study of the effects of very short thermal treatments at temperatures above those usually used for "activation" annealing may reveal new pathways for further optimizing Al_2O_3 passivation.

In this work, we make use of rapid thermal annealing (RTA) to investigate the effects of short, well-controlled thermal treatments on Al_2O_3 passivation over a wide temperature range. We investigate these effects for Al_2O_3 films deposited by atmospheric pressure chemical vapour deposition (APCVD), a simple technique well-suited to low-cost, high-throughput manufacturing. Photoconductance carrier lifetime and capacitance–voltage measurements are used to assess the quality of the passivation. We show that such short thermal treatments at moderate temperatures are capable of improving Al_2O_3 passivation beyond the level possible using conventional annealing treatments.

2. Experimental method

Symmetrically passivated Si–Al_2O_3 lifetime structures were prepared on ~480 μm thick 1 Ωcm *p*-type ⟨100⟩ float-zone Si wafers. These received a surface damage etch in HF:HNO_3 solution, followed by a standard RCA clean and dilute HF dip immediately prior to Al_2O_3 deposition. Additional metal–insulator–semiconductor (MIS) structures for capacitance–voltage (C–V) measurements were prepared on single-side-polished 2.8 Ωcm *p*-type and 1.3 Ωcm *n*-type ⟨100⟩ float-zone Si wafers. These received only an RCA clean and HF dip prior to deposition. Al_2O_3 films were deposited by APCVD from triethyldialuminium-tri-(*sec*-butoxide) (TEDA-TSB) and H_2O (H_2O:TEDA-TSB molar ratio of ~9:1) at substrate temperatures between 325 and 440°C [12]. The resulting film thickness varied with temperature, but was typically in the range of 10–12 nm. Some samples received a standard activation anneal at 425°C for 30 min in N_2 in a quartz tube furnace following deposition and prior to RTA. Rapid thermal annealing was performed in a UniTemp UTP-1100 oven employing infrared lamps at peak temperatures between 500 and 900°C for 1s in N_2 (40°C/s ramp rate). The sample temperature was monitored during annealing by a thermocouple in contact with the rear side of the sample.

Lifetime measurements were performed immediately following Al_2O_3 deposition and after each subsequent heat treatment. The effective excess carrier lifetime τ_{eff} was determined as a function of bulk excess carrier density Δn via inductively coupled photoconductance decay measurements using a Sinton Instruments WCT-120 system. Measurements were performed both with short flash illumination using the transient analysis and with quasi-steady-state illumination using the generalised analysis of [13], with the necessary optical constant determined by comparison with transient measurements for samples where these were possible.

Metal–insulator–semiconductor (MIS) samples for C–V measurements were formed following annealing by thermally evaporating Al through a shadow mask to form circular gate contacts (Ø ≈ 700 μm). GaIn eutectic paste was applied manually to form an ohmic rear contact. High-frequency (1 MHz) and quasi-static C–V measurements were performed using an HP 4284A precision LCR meter and HP 4140B picoammeter/DC voltage source. The

interface state density D_{it} was assessed from the quasi-static capacitance using the method of Berglund [14], while the fixed charge concentration Q_f was calculated from the measured flatband voltage shift. For full details of the experimental setup and analysis used, see [15].

Some additional Al_2O_3 passivation layers were prepared by atomic layer deposition (ALD) using a Beneq TFS-200 reactor. Both a thermal process using trimethylaluminium (TMA) and H_2O at 200°C and a plasma-assisted process with TMA and O_2 plasma at 175°C were used.

3. J_0 extraction

Surface passivation was assessed in terms of the surface saturation current density J_0, which has the advantage of being independent of both Δn and the bulk dopant density N_b, in contrast to the more commonly used effective surface recombination velocity S_{eff} [16]. In general, J_0 was calculated directly from the measured $\tau_{eff}(\Delta n)$ at $\Delta n = 10^{15}$ cm^{-3}, according to

$$J_0 = qn_i^2 \left(N_b + \Delta n\right)^{-1} \frac{W}{2}\left(\frac{1}{\tau_{eff}} - \frac{1}{\tau_{int}}\right), \tag{1}$$

where q is the fundamental electron charge, $n_i = 9.7\times10^9$ cm^{-3} is the intrinsic carrier concentration [17], W is the wafer thickness, and τ_{int} is the intrinsic bulk lifetime according to [18]. An alternative expression for J_0 may be derived by taking the derivative of (1) with respect to Δn (assuming J_0 is independent of Δn):

$$J_0 = qn_i^2 \frac{W}{2}\frac{d}{d\Delta n}\left(\frac{1}{\tau_{eff}} - \frac{1}{\tau_{int}}\right). \tag{2}$$

In general, excellent agreement was found between J_0 calculated from (1) and (2) for the examined samples.

Analysis of the data via (1) or (2) is complicated by the fact that contamination of the wafer bulk was also found to occur during the RTA step at higher temperatures. This is apparent from the fact that the resulting τ_{eff} exhibits a pronounced dip in low injection, characteristic of a Shockley–Read–Hall (SRH) recombination process. This reduced lifetime remains after stripping the original film and repassivating the surface, and is also observed for samples given an RTA prior to Al_2O_3 deposition. The lifetime could be recovered to close to its original value by applying a standard phosphorus gettering procedure [19], strongly suggesting the presence of metallic impurities. The magnitude of the lifetime reduction was found to increase with increasing RTA temperature, and was generally negligible at RTA temperatures of 550°C or below.

Comparison of $\tau_{eff}(\Delta n)$ before and after the application of strong illumination revealed that bulk iron contamination was definitely present, although neither interstitial iron (Fe_i) nor iron-boron pairs (FeB) are sufficient to explain all of the observed injection dependence, when using the parameters of [20, 21]. It was however found that the post-illumination lifetime data for all samples could be accurately modelled by assuming surface recombination described by a constant J_0 (i.e. low injection conditions at the silicon surface) and two bulk defects: one with the characteristics of interstitial iron (Fe_i) [20, 21], and one with a σ_n/σ_p ratio of 2.5. The resulting effective lifetime is described by the following equation:

$$\tau_{eff}^{-1} = \frac{J_0}{qn_i^2}\frac{2}{W}\left(N_b + \Delta n\right) + \tau_{int}^{-1} + \tau_{SRH,Fe_i}^{-1} + \tau_{SRH,2}^{-1}, \tag{3}$$

where τ_{SRH,Fe_i} and $\tau_{SRH,2}$ account for bulk SRH recombination via Fe_i defects and the second unidentified defect, respectively.

Fig. 1 illustrates the process of J_0 extraction via (3). For the samples measured prior to RTA, and for those measured after RTA at the two lowest peak temperatures (500 and 550°C), excellent agreement between the data and Equation (3) was obtained while neglecting the SRH terms, indicating negligible bulk contamination in these samples. Excellent agreement between J_0 calculated by Equations (1) and (2) was also obtained for these samples. For the other samples, J_0 was calculated by adjusting the concentration of the two bulk defect types in order to give good agreement both between Equation (3) and the measured τ_{eff}, and also between J_0 calculated from Equations (1) and (2). Fig. 2 shows the extracted bulk defect concentrations as a function of RTA peak temperature, assuming $\sigma_p = 10^{-15}$ cm^2 for the second defect. Despite some scatter, there is a clear trend of increasing bulk defect concentration with increasing RTA temperature, which is consistent with the diffusion of metallic contaminants. As this is clearly an extrinsic effect not related to the surface passivation, we do not consider it further here.

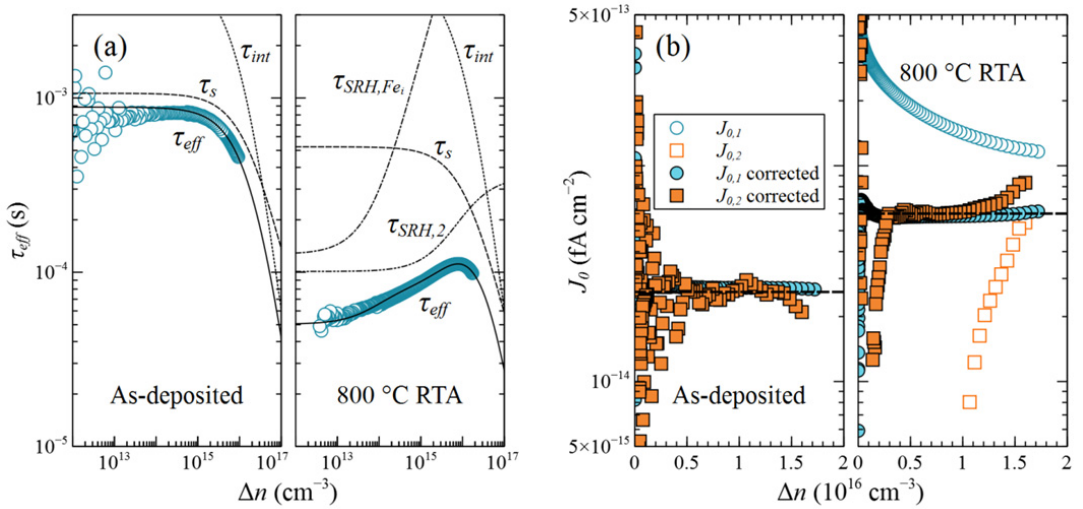

Fig. 1. (a) τ_{eff} and (b) J_0 as a function of Δn for an Al_2O_3-passivated sample (T_{dep} = 410°C, no anneal) before and after RTA at 800°C. The various contributions to τ_{eff} in Equation (3) are shown, along with J_0 calculated from both Equation (1) ($J_{0,1}$) and Equation (2) ($J_{0,2}$). Prior to RTA, τ_{eff} is well-described by Equation (3) without the SRH terms, and $J_{0,1}$ and $J_{0,2}$ agree closely without the need for any corrections. After RTA, significant bulk contamination is present, and $J_{0,1}$ and $J_{0,2}$ diverge. The bulk SRH components are determined such that good agreement is achieved between $J_{0,1}$ and $J_{0,2}$ calculated from the corrected τ_{eff}. Dashed lines show the extracted J_0 values in each case.

4. Results and discussion

As shown in Fig. 3, J_0 may either decrease or increase following RTA relative to the as-deposited value, depending on both the deposition and RTA temperatures, but in general increases with the latter. Clear transition points in post-RTA J_0 are apparent around 600°C and above 800°C, which is consistent with earlier reports, and with the out-diffusion of hydrogen- and oxygen-containing species observed at these temperatures during thermal effusion measurements [22], indicating structural modifications of the bulk film and/or interface.

For films deposited at temperatures of 325 and 355°C, J_0 as-deposited is rather high, but improves substantially upon RTA. An optimum RTA temperature exists within the examined range, and this shifts to lower temperatures as deposition temperature increases. For the films deposited at 385°C, J_0 as-deposited is quite variable, because the deposition temperature is in the transition region where substantial changes in interface quality occur [12]. J_0 after RTA is generally substantially reduced, except in the case of RTA temperatures greater than 800°C, and displays much less random variation, increasing monotonically with RTA temperature. As the deposition temperature increases further to 410°C, the as-deposited J_0 stabilises at a significantly lower level, while the RTA temperature above which J_0 increases rather than decreases after RTA is reduced to between 600 and 650°C. The inclusion of a standard anneal prior to RTA initially reduces J_0, but results in somewhat higher post-RTA J_0. At a deposition

temperature of 440°C, J_0 is no longer significantly reduced by annealing, and is significantly increased by RTA at temperatures of 600°C or above.

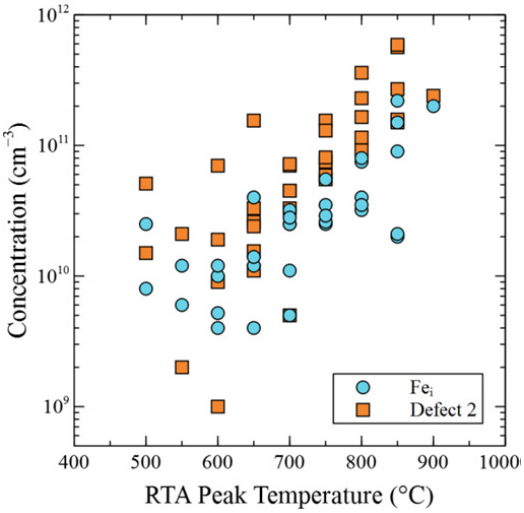

Fig. 2. Bulk concentration of Fe_i and the second, unidentified defect as a function of RTA peak temperature, as determined during J_0 extraction using Equation (3). $\sigma_p = 10^{-15}$ cm^2 is assumed for the second defect.

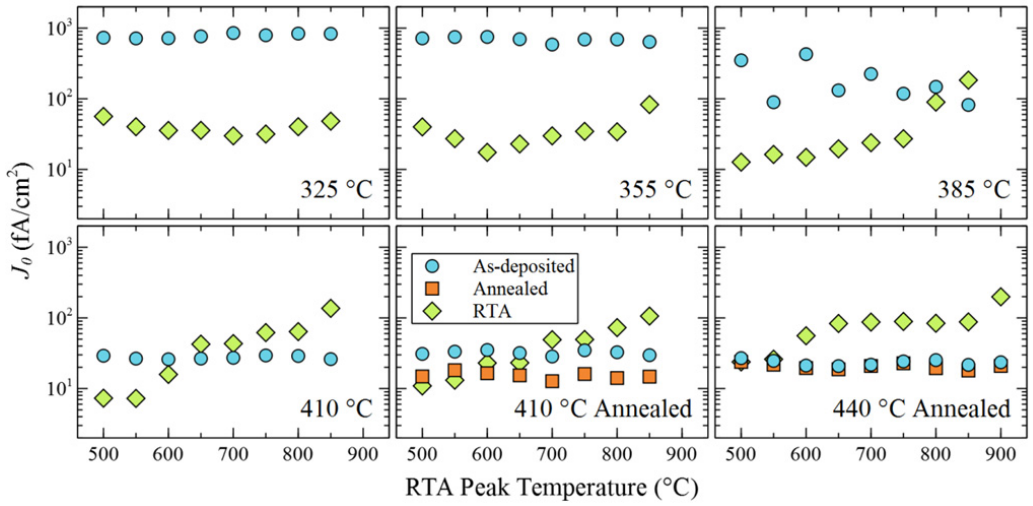

Fig. 3. J_0 as a function of RTA peak temperature for Al_2O_3 films deposited at various temperatures (indicated in each subfigure) on undiffused 1 Ωcm *p*-type ⟨100⟩ Si surfaces, with or without an intermediate anneal at 425°C in N_2. J_0 values are shown for the films as-deposited, after annealing (if applicable), and after RTA.

Fig. 4 shows post-RTA J_0 in the form of a contour map, as a function of both Al_2O_3 deposition temperature and RTA peak temperature. Fig. 4 shows clearly that the optimum Al_2O_3 deposition temperature (in terms of minimising J_0) depends strongly on the post-deposition thermal processing to be applied. For RTA peak temperatures between 500 and 600°C, the optimum deposition temperature occurs at 410°C. As RTA peak temperature increases, the optimum deposition temperature decreases, falling to ~350°C at an RTA peak temperature of 800°C.

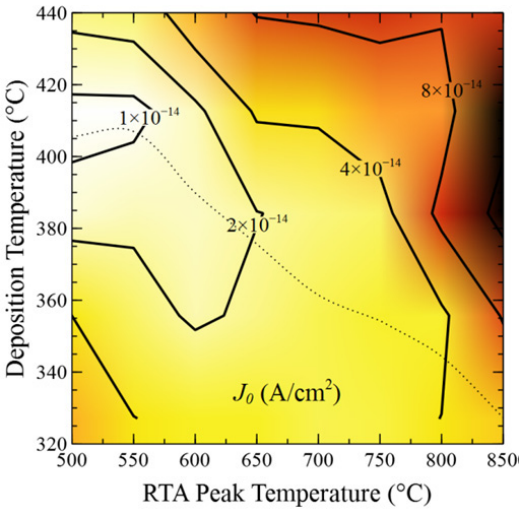

Fig. 4. Contour map of post-RTA J_0 as a function of RTA peak temperature and Al_2O_3 deposition temperature, derived from the data of Fig. 3. The dotted line shows the deposition temperature corresponding to the minimum value of post-RTA J_0 at a given RTA peak temperature

Al_2O_3 films deposited at higher temperatures display excellent passivation following low-temperature RTA heat treatment, but their passivation quality degrades substantially at higher RTA temperatures. Conversely, films deposited at lower temperatures require moderate heat treatment to reach their minimum J_0 values, which are not as low as those of higher temperature films, but maintain their passivation quality over a broader and higher range of RTA temperatures. This difference in thermal stability may be related to the greater hydroxyl content of the low-temperature films [15], or perhaps more generally to the greater thermal budget required for the structural transitions involved in passivation and depassivation of the surface.

Most interestingly, a minimum J_0 of 7 fA cm^{-2}, significantly lower than that obtained by conventional annealing, is observed for Al_2O_3 films deposited at ~410°C after RTA at 500 or 550°C. This represents an exceptionally good level of surface passivation, and prompts an investigation of the interface properties of these films. C–V measurements of identically prepared MIS structures (Fig. 5) reveal that after RTA, D_{it} is reduced by a factor of two, from 11×10^{10} eV^{-1} cm^{-2} to ~5×10^{10} eV^{-1} cm^{-2}. A similar reduction of D_{it} occurs upon extended (30 minutes) annealing at 425°C in N_2. However, while the longer, lower temperature anneal results in an increase in negative Q_{tot} to -2.0×10^{12} cm^{-2} from its as-deposited value of -1.2×10^{12} cm^{-2}, the RTA results in a significantly larger increase, to $Q_{tot} = -3.3\times10^{12}$ cm^{-2}. This combination of remarkably low D_{it} and large Q_{tot} accounts for the exceptionally low J_0 of surfaces passivated by these films.

In order to show even more clearly the high quality of the passivation layers prepared in this way, Fig. 6 compares τ_{eff} vs Δn measured with these films, both as-deposited and after either a standard furnace anneal or an optimised RTA treatment, with that of identical substrates passivated by Al_2O_3 prepared by standard thermal and plasma-assisted ALD processes. The latter are considered to provide a benchmark for surface passivation quality, where the plasma process is known to yield better results, but is less industrially relevant. Following a standard extended anneal, the APCVD Al_2O_3 layer performs well, but does not quite reach the level of the thermal ALD film. However, if an optimised RTA is applied in place of the standard anneal, τ_{eff} of the APCVD-passivated sample surpasses that of the thermal ALD case. This impressive result shows that CVD processes are capable of forming Al_2O_3 layers of exceptionally high quality, matching or exceeding that of similar layers prepared by state-of-the-art thermal ALD processes. It also shows the importance of optimising the post-deposition thermal processing to maximise the potential of the deposited layers.

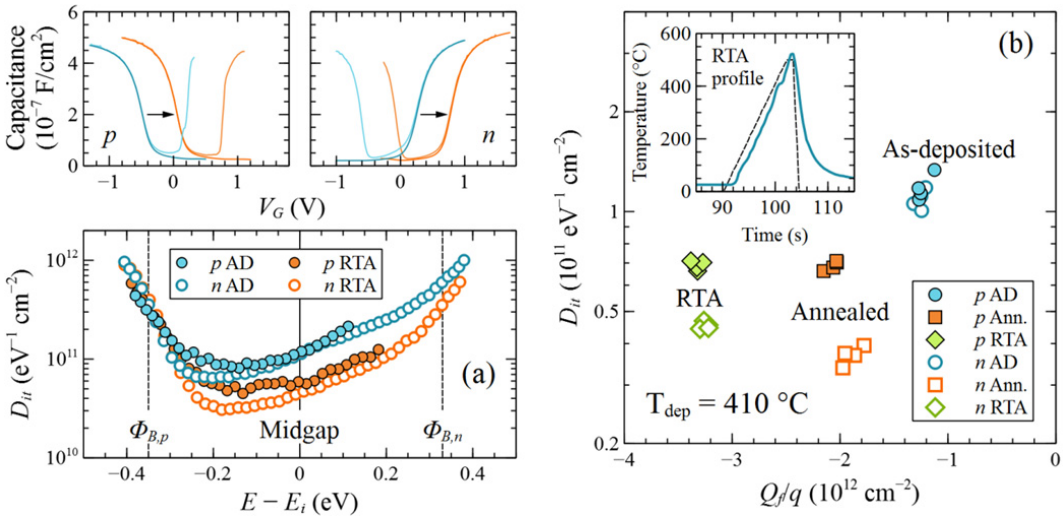

Fig. 5. a) Typical C–V characteristics and resulting D_{it} distribution for Al_2O_3 deposited on *p*- and *n*-type substrates at ~410°C, as-deposited and after RTA at 500°C. b) Midgap D_{it} vs Q_f determined from multiple such measurements at different points on the same samples, both as-deposited, and after either annealing at 425°C in N_2, or RTA at 500°C. Inset shows the measured (solid) and set (dashed) RTA temperature profile.

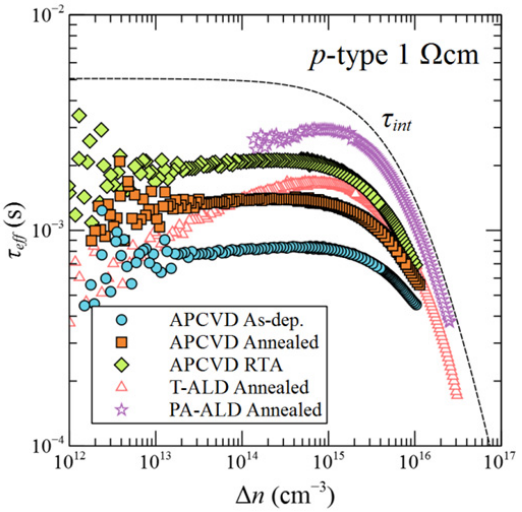

Fig. 6. τ_{eff} vs Δn for 480 µm thick *p*-type 1 Ωcm ⟨100⟩ FZ-Si wafers passivated by APCVD Al_2O_3 films deposited at 410°C, both as-deposited and after either a standard 30 min anneal at 425°C in N_2, or an RTA at 500°C. Data are also shown for the same wafers passivated by Al_2O_3 prepared by thermal ALD (200°C, 20 nm, annealed for 30 min at 425°C in N_2) and plasma-assisted ALD (175°C, 20 nm, annealed for 15 min at 425°C in 5% H_2 in Ar).

The degradation of J_0 observed at higher RTA temperatures appears to conflict with previous results on the firing stability of the Al_2O_3 passivation. In previous work [11], we observed passivation to improve following a conventional fast-firing step in a belt furnace with peak substrate temperature over 800°C. Conversely, a much shorter RTA step at a similar temperature was found to result in a significant deterioration of passivation quality for the same films and substrates. The reason for this apparent discrepancy may be related to the different heating methods employed by the two processes, which in the case of RTA involves high-intensity illumination of the substrate by infrared lamps, which at high intensity can have significant emission in the UV [23]. Such illumination

has previously been linked to surface passivation degradation observed for SiO_2-passivated surfaces during RTA [23]. It is therefore possible that the observed degradation is related to the presence of this illumination rather than being a purely thermal process. Further work is necessary to clarify this question.

It is possible that the illumination also plays a role in the passivation improvement observed at lower temperatures. It is known that strong illumination with higher-energy photons may induce an increase in the Al_2O_3 fixed charge Q_f [24], which would be consistent with the strong increase observed in Fig. 5. If this were the case it would raise interesting questions regarding other previous results, since a number of previous works have employed similar RTA systems to perform their activation anneals.

5. Conclusions

Systematic investigation of the effects of post-deposition heat treatment by RTA on Al_2O_3 surface passivation reveals a number of trends. J_0 post-RTA may either increase or decrease depending on Al_2O_3 deposition temperature and RTA peak temperature, but generally increases with the latter. The optimum deposition temperature depends on the post-deposition thermal processing to be applied. Films deposited at lower temperatures provide worse passivation after low temperature heat treatment, but maintain this passivation better at higher RTA temperatures. Al_2O_3 passivation exposed to RTA at high temperatures exhibits a degradation that is not observed for similar films exposed to a conventional fast-firing process at the same temperature, pointing to the possible influence of non-thermal effects in the degradation process. On the other hand, RTA at more moderate temperatures can result in passivation improvements beyond those possible with a standard extended anneal at 425°C. An exceptionally low J_0 of 7 fA/cm^2, due to a combination of very low D_{it} and unusually high Q_f, is achieved by the use of a short 500–550°C RTA combined with optimised deposition conditions. It is shown by direct comparison that this passivation is as good as or better than that of Al_2O_3 prepared by a standard thermal ALD process, demonstrating the outstanding passivation potential of Al_2O_3 prepared by relatively simple CVD processes, as well as the potential gains of optimising the post-deposition thermal treatment.

Acknowledgements

The authors would like to thank Wensheng Liang for providing the lifetime data for plasma-assisted ALD Al_2O_3, and Pheng Phang for assistance with phosphorus gettering.

References

[1] A. Richter, S. W. Glunz, F. Werner, J. Schmidt, and A. Cuevas, "Improved quantitative description of Auger recombination in crystalline silicon", Physical Review B 86, 165202 (2012).
[2] A. Richter, J. Benick, M. Hermle, and S. W. Glunz, "Excellent silicon surface passivation with 5 Å thin ALD Al_2O_3 layers: Influence of different thermal post-deposition treatments", Physica Status Solidi RRL 5, 202–204 (2011).
[3] B. Vermang, H. Goverde, A. Lorenz, A. Uruena, G. Vereecke, J. Meerschaut, E. Cornagliotti, A. Rothschild, J. John, J. Poortmans, and R. Mertens, "On the blistering of atomic layer deposited Al_2O_3 as Si surface passivation", Proceedings of the 37th IEEE Photovoltaic Specialists Conference, Seattle, Washington, USA, 2011, pp. 3562–3567.
[4] F. Kersten, A. Schmid, S. Bordihn, J. W. Müller, and J. Heitmann, "Role of annealing conditions on surface passivation properties of ALD Al2O3 films", Energy Procedia 38, 843–848 (2013).
[5] W. Liang, K. J. Weber, and A. F. Thomson, "Effective SiNx:H capping layers on 1-nm Al2O3 for p+ surface passivation", IEEE Journal of Photovoltaics 4, 1405–1412 (2014).
[6] A. Richter, J. Benick, and M. Hermle, "Boron emitter passivation with Al2O3 and Al2O3/SiNx stacks using ALD Al2O3", IEEE Journal of Photovoltaics 3, 236–245 (2013).
[7] J. Benick, A. Richter, M. Hermle, and S. W. Glunz, "Thermal stability of the Al2O3 passivation on p-type silicon surfaces for solar cell applications", Physica Status Solidi RRL 3, 233–235 (2009).
[8] B. Veith, F. Werner, D. Zielke, R. Brendel, and J. Schmidt, "Comparison of the thermal stability of single Al2O3 layers and Al2O3/SiNx stacks for the surface passivation of silicon", Energy Procedia 8, 307–312 (2011).
[9] P. Saint-Cast, D. Kania, R. Heller, S. Kuehnhold, M. Hofmann, J. Rentsch, and R. Preu, "High-temperature stability of c-Si surface passivation by thick PECVD Al2O3 with and without hydrogenated capping layers", Energy Procedia 258, 8371–8376 (2012).

[10] D. Schuldis, A. Richter, J. Benick, and M. Hermle, "Influence of different post deposition treatments on the passivation quality and interface properties of thermal ALD Al2O3 capped by PECVD SiNx", Proceedings of the 27th European Photovoltaic Solar Energy Conference, Frankfurt, Germany, 2012, pp. 1933–1937.
[11] L. E. Black, T. Allen, A. Cuevas, K. R. McIntosh, B. Veith, and J. Schmidt, "Thermal stability of silicon surface passivation by APCVD Al2O3", Solar Energy Materials and Solar Cells 120, 339–345 (2014).
[12] L. E. Black, and K. R. McIntosh, "Surface passivation of c-Si by atmospheric pressure chemical vapor deposition of Al2O3", Applied Physics Letters 100, 202107 (2012).
[13] H. Nagel, C. Berge, and A. G. Aberle, "Generalized analysis of quasi-steady-state and quasi-transient measurements of carrier lifetimes in semiconductors", Journal of Applied Physics 86, 6218–6221 (1999).
[14] C. N. Berglund, "Surface states at steam-grown silicon-silicon dioxide interfaces", IEEE Transactions on Electron Devices 13, 701–705 (1966).
[15] L. E. Black, "New perspectives on surface passivation: understanding the Si–Al2O3 interface", PhD Thesis, The Australian National University (2015).
[16] K. R. McIntosh and L. E. Black, "On effective surface recombination parameters", Journal of Applied Physics 116, 014503 (2014).
[17] K. Misiakos and D. Tsamakis, "Accurate measurements of the silicon intrinsic carrier density from 78 to 340 K", Journal of Applied Physics 74, 3293–3297 (1993).
[18] A. Richter, S. W. Glunz, F. Werner, J. Schmidt, and A. Cuevas, "Improved quantitative description of Auger recombination in crystalline silicon", Physical Review B 86, 165202 (2012).
[19] S. P. Phang and D. Macdonald, "Direct comparison of boron, phosphorus, and aluminum gettering of iron in crystalline silicon", Journal of Applied Physics 109, 073521 (2011).
[20] D. Macdonald, T. Roth, and P. N. K. Deenapanray, "Doping dependence of the carrier lifetime crossover point upon dissociation of iron-boron pairs in crystalline silicon", Applied Physics Letters 89, 142107 (2006).
[21] D. Macdonald, J. Tan, and T. Trupke, "Imaging interstitial iron concentrations in boron-doped crystalline silicon using photoluminescence", Journal of Applied Physics 103, 073710 (2008).
[22] G. Dingemans, P. Engelhart, R. Seguin, F. Einsele, B. Hoex, M. C. M. Van de Sanden, and W. M. M. Kessels, "Stability of Al2O3 and Al2O3/a-SiNx:H stacks for surface passivation of crystalline silicon", Journal of Applied Physics 106, 114907 (2009).
[23] T. C. Kho, L. E. Black, and K. R. McIntosh, "Degradation of Si–SiO2 interfaces during rapid thermal annealing", in Proceedings of the 24th European Photovoltaic Solar Energy Conference, 21–25 September, Hamburg, Germany, 1586–1590 (2009).
[24] R. Hezel and K. Jaeger, "Low-temperature surface passivation of silicon for solar cells", Journal of the Electrochemical Society 136, 518–523 (1989).